

JOINT TRAJECTORY OPTIMIZATION AND DECONFLICTION FOR CLIMATE IMPACT MITIGATION

Thorsten Ehlers[1], Alexander Lau[1], Max Mendiguchia Meuser[1], Alexander Kuenz[2], Simone Dietmüller[3] & Sigrun Matthes[3]

[1]Institute of Air Transport, German Aerospace Center
[2]Institute of Flight Guidance, German Aerospace Center
[3]Institute of Atmospheric Physics, German Aerospace Center

Abstract

Optimizing individual trajectories has shown great potential in reducing the non-CO_2 climate impact of aviation [1] [2]. However, these optimized flight trajectories must be designed in a way that ensures conflict-free operation in accordance with given minimum separations. Otherwise, their safe implementation in operational environments cannot be ensured. Initial results of deconflicted climate-impact mitigation trajectories in a free-flight scenario using the trajectory optimizer pyTOM [3] as well as the deconfliction tool NDMap [4] are provided. These results indicate that an *optimize-first - deconflict-later* approach can generate conflict-free traffic scenarios while preserving a large share of the individual climate mitigation potential achieved through trajectory optimization. Ideally, trajectory optimization and conflict resolution are performed within an iterative process that enables flexible adaptation to changing external conditions, like e.g. aligned to uncertain climate sensitive airspaces. Climate impact mitigation for individual trajectories must be addressed throughout the entire trajectory life cycle, from initial planning and short-term adjustments of the filed business trajectory to the in-flight phase. This study focuses on achieving both conflict-free operations and the reduction of each trajectory's climate impact to a desired minimum.

Keywords: Trajectory; Meteorology; convective weather; single flight optimization; flight trajectories

1. Introduction

The climate impact of aviation stems from CO_2 emissions and non-CO_2 effects caused by Ozone and Methane induced by the emission of nitrogen oxides (NO_X), the formation of persistent contrail-induced clouds (CiC), the emission of water vapour and other species. Persistent contrails can form in ice-supersaturated regions (ISSRs), i.e., areas where the relative humidity with respect to ice exceeds 100% and the temperature falls below the frost point, thus providing conditions favorable for the nucleation and persistence of ice crystals. Examples of those regions are shown in Figure 4a. Thus, in order to reduce aviation's climate impact it appears promising to avoid ISSRs either laterally or vertically. Trajectory optimization with the target of minimizing CiC formation is inherently challenging, as it requires accurate forecasts of regions where persistent contrails are likely to form. Moreover, a trade-off must be balanced between increased direct operating costs (DOC) and additional emissions resulting from detours, and the potential reduction in climate impact achieved by mitigating non-CO_2 effects. Furthermore, the airspace is shared by a large number of aircraft operating simultaneously. To ensure a safe operation, aircraft must be separated according to minimum separation margins at any time. In this paper, we propose an iterative trajectory optimization with a subsequent conflict resolution approach that enables climate-optimal routing while ensuring safe aircraft operations. Our study analyses to what extent deconflicting results in trajectories being redirected back into climate-sensitive airspaces, potentially inhibiting the intended reduction in climate effects.

2. Related Work

The climate impact of aviation arising from both CO_2 and non-CO_2 effects has been investigated by Lee et al. [5], showing that non-CO_2 effects form a significant share of aviation's climate impact. The climate impact of individual species, e.g. NO_x-induced changes in ozone and methane or contrail-induced cirrus clouds, is a field of activate research [6, 7]. In the project D-Kult (Demonstrator Climate and Environmentally Friendly Air Transport) [8], the impact of adapting trajectories for avoiding CiC was investigated by adapting trajectories of real flights. The results of these studies help improving first-order models like Algorithmic Climate Change Functions (aCCFs) [9, 10, 11]. These Algorithmic Climate Change Functions provide a computationally efficient method for estimating the spatially and temporally resolved non-CO_2 climate effects of aviation emissions as a function of the prevailing atmospheric conditions. Unlike conventional trajectory optimization metrics based solely on fuel burn or CO_2 emissions, aCCFs also account for non-CO_2 effects. By linking meteorological data with emission sensitivities, they enable the identification of climate-sensitive regions and support climate-optimized trajectory planning. This allows aircraft routes to be adapted dynamically in order to reduce the overall climate impact of aviation while maintaining operational feasibility. They are often used in research focusing on mitigating specific non-CO_2 effects [12]. An implementation of aCCFs is provided by the open source tool CLIMaCCF [10, 11].

However, reducing climate impact is not the only goal when optimizing trajectories. Most importantly, they have to be safe, but also economically viable in terms of cost efficiency. Lau et al. [13] introduced a two-stage framework in which a graph-based routing approach is used to generate feasible trajectories that circumvent climate-sensitive airspace and restricted regions such as convective cells. These trajectories are subsequently refined using an optimal control algorithm, optimizing a multi-criteria cost function which seeks to balance operating costs and climate impact while ensuring a safe trajectory.

Such optimizations are typically performed on individual trajectories. As flights share the same airspace, they must be managed in a way that prevents violations of separation minima. Such conflict-free scenarios can be computed by using DLR's real-time conflict detection and resolution suite for air traffic management N-Dimensional Map (NDMap).

The aim of this paper is to combine these two perspectives of optimizing single trajectories, and finding a conflict-free flight plan.

3. Methodology

In this section, we detail the single components of optimizing trajectories, resolving conflicts, and combining these two fields for obtaining optimized, conflict-free mitigation trajectories.

3.1 Wind and Convective Cells

Wind plays an important role for the design of efficient flight trajectories. Wind data and the relevant input parameters for computing aCCFs were extracted from European Centre for Medium-Range Weather Forecasts (ECMWF) re-analysis data ERA5 [14]. An example of wind speed and direction is presented in Figure 1.

For a more realistic and operationally relevant setup, convective cells were incorporated into the experiments based on Cb-Global data [15], accounting for the significant influence of convection on flight routing and conflict resolution. Each cell is associated with a sigmoid-shaped penalty function, which generates a gradient to steer the trajectory optimization process.

Figure 2a shows an example of convective cells, shown as red polygons, in Europe. Their translation into a cost function is shown in Figure 2b together with an exemplary trajectory between Madrid (MAD) and Tel Aviv (TLV). A flight route on the great circle, shown in grey, would cross the convective cells over the Aegaen Sea, whereas an optimized trajectory, shown in red, avoids it, also keeping a safety margin. This margin is not enforced, but incentivized by the cost function.

3.2 Climate Effect

The climate impact assessment is carried out using algorithmic Climate Change Functions (aCCFs) Version 1.0A [9, 11], which provide spatially and temporally resolved estimates of individual non-CO_2

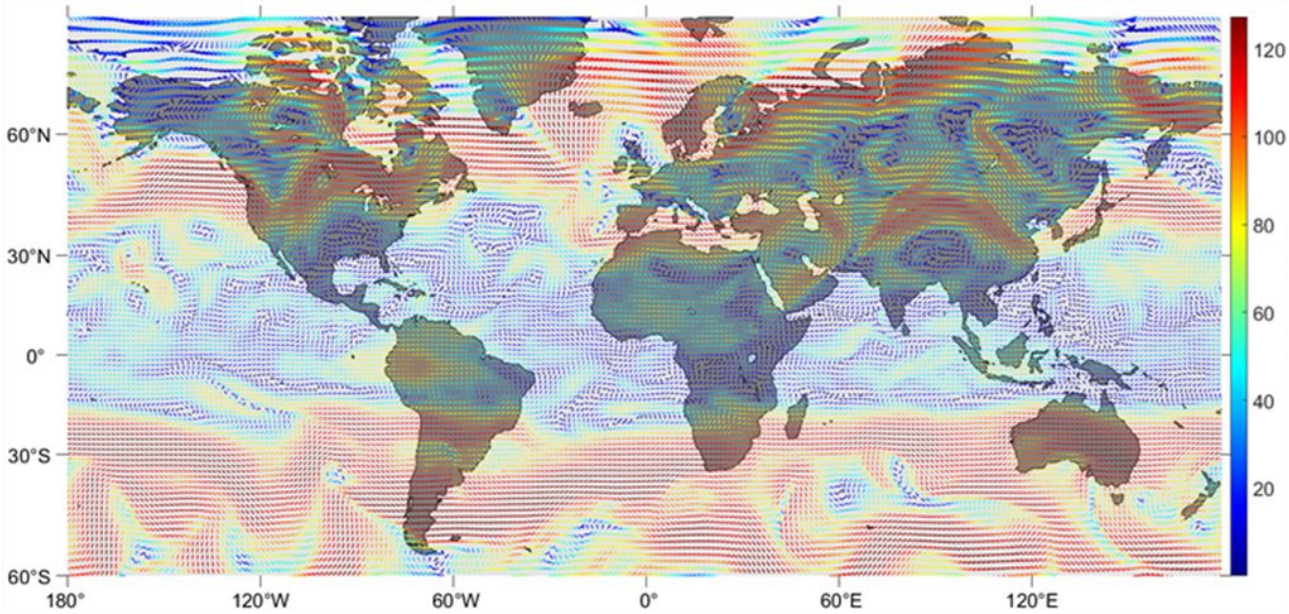
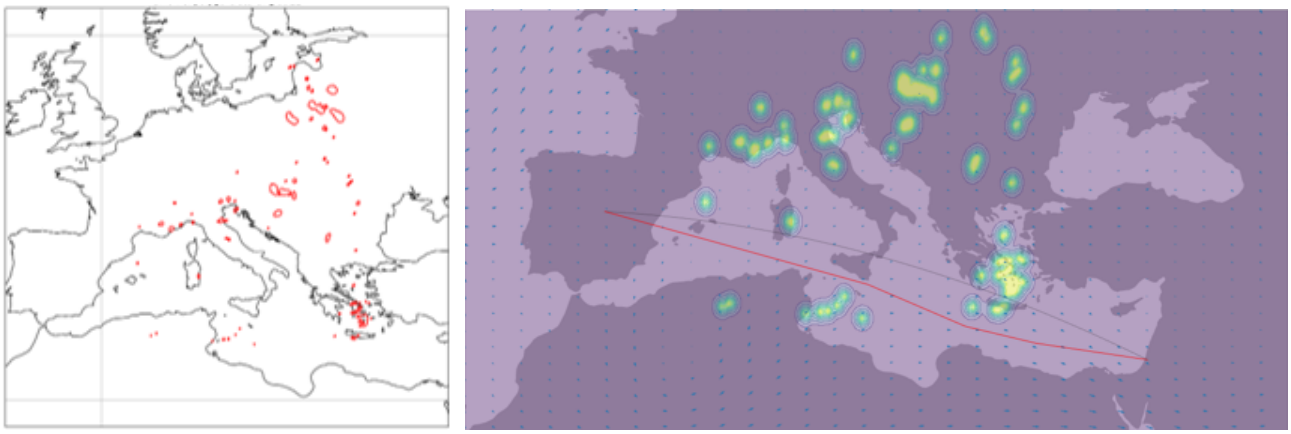


Figure 1 – Example for Global Wind Speed and direction on FL 350

climate effects, including the NO_x-induced ozone (warming impact) and methane effect (cooling impact), water vapour (warming) and contrails (both warming and cooling). They are represented by simple, statistically derived, mathematical functions that use local meteorological parameters at time of emission as input data, including geopotential, temperature, outgoing longwave radiation, relative humidity over ice, and potential vorticity. These functions were derived for typical summer and winter conditions and are limited over the North Atlantic Flight Corridor for pressure levels 200-400 hPa. Thus, their application outside this design-region is possible, however, they are only calibrated for this region. With the Python-based open-source library CLIMaCCF [10], a technical implementation for calculating individual and merged aCCF is provided. In this study aCCFs are described as Future Average Temperature Response over a time horizon of 50 years (F-ATR-50). Contrail, water vapour and NO_x-induced (combination of methane and ozone) aCCFs are shown in Figure 4. The figures demonstrate that NO_x-related climate effects distributed on a broad spatial scale with relatively smooth gradients, while the climate effect of contrail-induced cirrus (CiC) is concentrated to contrail-forming regions and exhibits strong spatial variability. This localized nature makes CiC effects more responsive to mitigation through optimized routing strategies.
As the individual aCCF are given in different units (i.e.,K/kg(NO_2) for the NOx aCCFs, K/km for the CiC aCCF and K/kg(fuel) for the water vapour aCCF), they are converted to K/kg(fuel) using average emission indices and a "merged non-CO_2 aCCF" can be generated (Figure 3). This yields a climate cost function which only depends on the fuel flow.

3.3 Trajectory Optimization

Following [3], we employ our trajectory optimization framework *pyTOM*. The process begins with the computation of a route using a graph-based approach, which is optimized with respect to a multi-criteria objective that minimizes direct operating costs (DOC) and climate impact while additionally accounting for safety constraints such as the avoidance of convective cells. We use a simple grid as a graph, where the nodes are formed as tuples of integer latitude and longitude values. Directly computing a path on this graph would result in a zig-zag pattern. There are mainly two ways to create a smooth path on such graphs. Firstly, a post-processing step can be used in order to smoothen the result. However, results from this approach tend to be sub-optimal as the search space is severly limited [16]. Thus, we use a theta* algorithm [17] to ensure that the result is relatively smooth and serves as a good initial guess for the optimal control algorithm. The resulting route is then augmented with a vertical profile and used as an initial guess for an optimal control problem. Here, a total energy model [18] is used as shown in Equation 1. It states that if the thrust provided by the engines is larger



(a) Example for convective cells

(b) Cost function representing convective cells. The usage of a sigmoid function creates areas around the convective cells which are also penalized.

Figure 2 – Convective cells, and their implementation in a penalty term used by the optimizer. The penalty term incentivizes the optimizer to choose a route which keeps some margin to the convective cells.

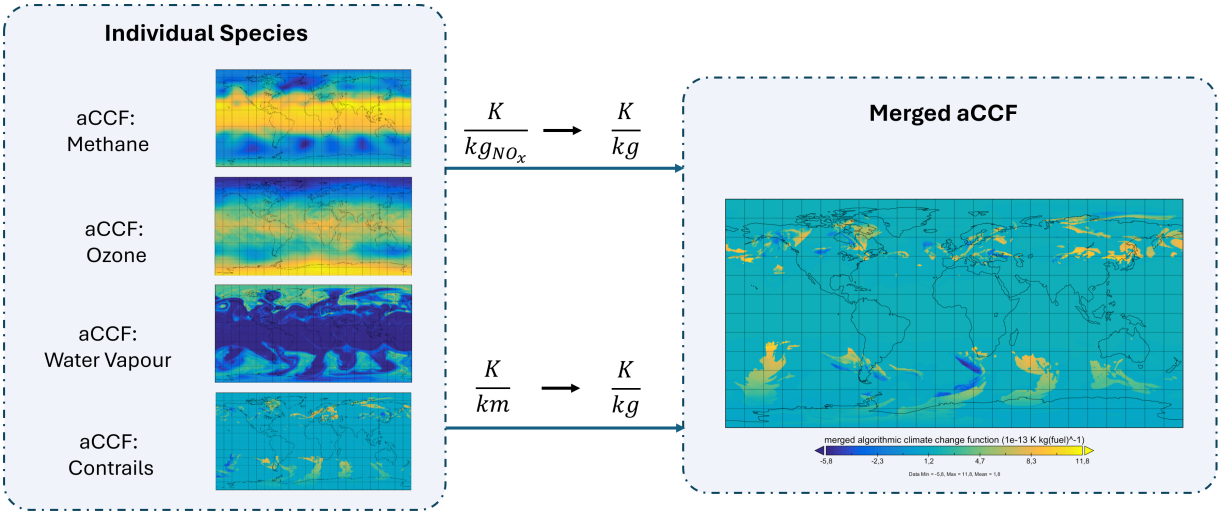


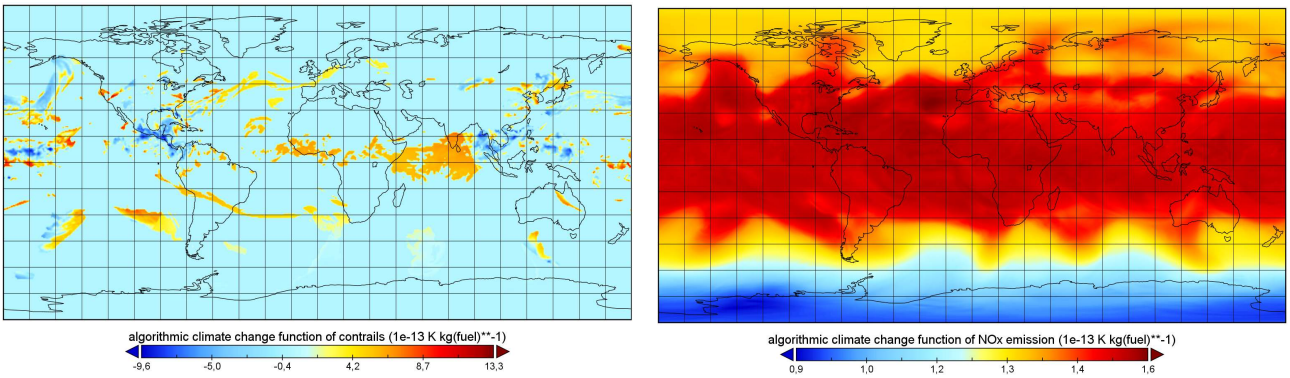
Figure 3 – Derivation of the overall non-CO_2 climate effect from the individual species methane, ozone, water vapour, and CiC.

than the drag, the resulting power surplus can be used for acceleration or climbing.

$$v_{TAS}(thrust - drag) = m\frac{dv_{TAS}}{dt}v_{TAS} + mg\frac{dh}{dt} \tag{1}$$

$$costs = \int_{t=0}^{t_f} \sum_{c\in\{DOC,accf,cb\}} w_c c\,(\lambda(t), \varphi(t), h(t), ff(t), t) \tag{2}$$

The cost function is given in Equation 2, where $\lambda(t)$ and $\varphi(t)$ denote the longitude and latitude at time t, $h(t)$ is the height, and $ff(t)$ denotes the fuel flow at time t. We solve the multi-objective optimization problem by minimizing costs given as the sum of different cost functions, each of them with a weight w_c. While the weight for avoiding convective cells (cb) is chosen sufficiently high such that these cells are avoided, the weights of DOC and climate impact can be varied to prioritize one over the other, or find solutions which seek to reduce the climate impact while still being efficient in terms of DOC. This optimal control problem is solved using Dymos [19] with SLSQP as optimizer, and a pseudospectral transcription. Here, aircraft dynamics are parameterized with BADA4 data [18].
Figure 5 shows the impact of this approach, where convective cells are shown in red, and climate sensitive areas in green (high impact) and blue (low impact): If the great circle is used as initial



(a) Climate impact of contrail-induced cirrus clouds

(b) Climate impact of NO_X emissions

Figure 4 – Example of algorithmic climate change functions illustrating the climate effect (K/kg(fuel)) of contrail-induced cirrus (CiC) and NO_x emissions for June 16th, 2018 at 00:00z at pressure level 200 hPa. The climate-sensitive airspace associated with CiC exhibits a well-defined spatial structure (left), whereas the NO_x-induced climate effect is distributed over larger regions, resulting in comparatively flat gradients for optimization purposes.

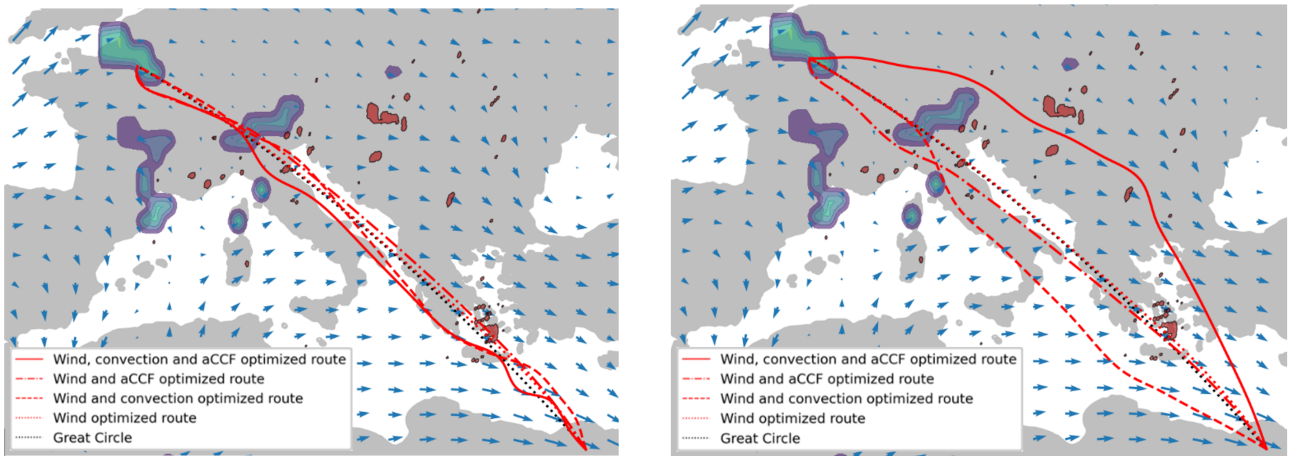
solution, the optimal control optimizer is stuck in a local optimum which it cannot escape, as can be seen in Figure 5a. On the contrary, the routes computed by the graph-based approach avoid both the climate sensitive regions and the convective cells. Using them yields better results from the continuous optimization, c.f. Figure 5b.
Free Vertical Planning (FVP) as a related concept removes fixed vertical constraints and allows continuous vertical optimization of aircraft trajectories, which can improve fuel efficiency and enable more flexible trade-offs between wind, CiC avoidance, and conflict mitigation while maintaining current separation standards [20].

3.4 Deconfliction

After the individual trajectories have been optimized, conflict resolution is performed following the approach in [21], using *NDMap*. Although the *NDMap* is also capable of detecting conflicts between flights and no-fly-zones, this paper is restricted to inter-flight conflicts. Violations are detected based on well-defined separation minima (Figure 6a) and resolved using multiple strategies:

- Temporal adjustments can be applied both, forward and backward in time, and recursively if necessary, until all separation constraints are satisfied. Currently, flights are shifted by up to ± 10 minutes.
- Lateral resolution is applied to pass in front of or behind the conflict partner (Figure 6b).
- Vertical resolution solves a separation violation by climbing above or diving below the conflict partner (Figure 6c).

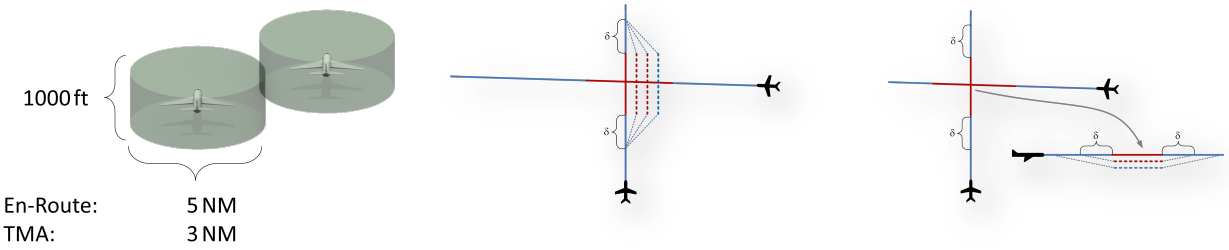
Lateral and vertical resolution algorithms both keep the remaining route stable by adapting the δ accordingly. Only the time dimension is adapted after merging back on the initial route to respect the additional time necessary for the detour.
All resolution algorithms follow an intelligent trial-and-error approach, benefiting from the high conflict detection performance. On average, all conflicts of one single trajectory with all other trajectories are detected in about 2 ms, with a low dependency of scenario's size and density. Deletion of a trajectory takes about 1 ms, summing up to 3 ms for a complete trial-and-error cycle. That way, the conflict resolution performs more than 300 trials per second. A trial is successful, if the trajectory resolves the conflict *and* does not create new conflicts further downstream. Valid resolutions are directly implemented, and the *NDMap* continues with the chronologically next conflict.



(a) Great Circle Used as Initial Solution: The trajectories pass between two climate-sensitive regions over northern Italy. The optimizer is not able to escape from this local minimum.

(b) Optimized Route Used as Initial Solution. The routes optimized for aCCF avoid the climate sensitive region over northern Italy.

Figure 5 – Impact of Using Optimized Initial Solutions for Optimal Control. Convectice cells are marked in red, and climate sensitive regions in green (high impact) and blue (lower impact).



(a) Separation Minima

(b) Lateral Deconfliction

(c) Vertical Deconfliction

Figure 6 – Deconfliction using NDMap

3.5 Iterative Approach

In this paper, we use an iterative approach which combines the optimization of individual trajectories with deconfliction as shown in Figure 7. First, individual trajectories are optimized such that convective cells are avoided, and both DOC and climate impact are minimized. Due to the individual trajectory optimization, it is likely that there will be conflicts between the resulting trajectories, i.e. cases in which separation minima are violated. Thus, the deconfliction routine is used to resolve these conflicts, moving parts of the flight trajectories laterally or vertically, or shifting them in time. This will resolve the conflicts, however, there is a risk that optimizations will be undone, i.e. trajectories might get pushed into climate sensitive zones, increasing their climate impact, or in convective cells, which must be avoided due to safety reasons. Therefore, we iterate these two processes of trajectory optimization and deconfliction until both the climate impact is minimized, and there are no conflicts left. This process can always be stopped after deconfliction, however, the research question arising here is: Does this still yield good results in terms of climate impact minimization?

3.6 Use Case

For the evaluation of the "optimize first, deconflict later"-approach, a traffic scenario was chosen which contains all flights touching the European Civil Aviation Conference (ECAC) airspace between 12am and 4pm on a summer day, June 16^{th}, 2018, and a winter day, December 11^{th}, 2018. The flights from the summer day are shown in Figure 8. These scenario days contain 8661 and 7299 flights, respectively. While the majority of these flights originates and ends inside Europe, some originate or end outside the continent.

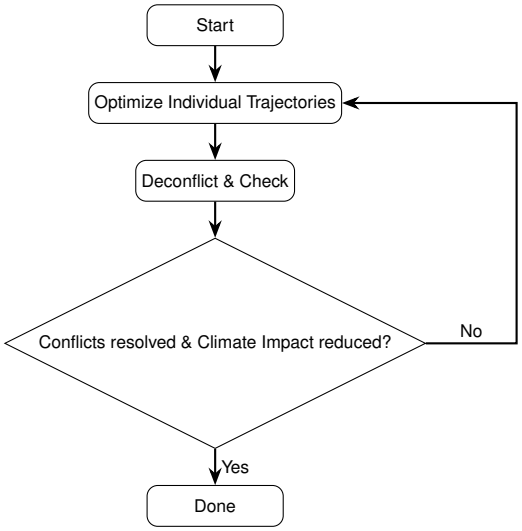


Figure 7 – Iterative approach

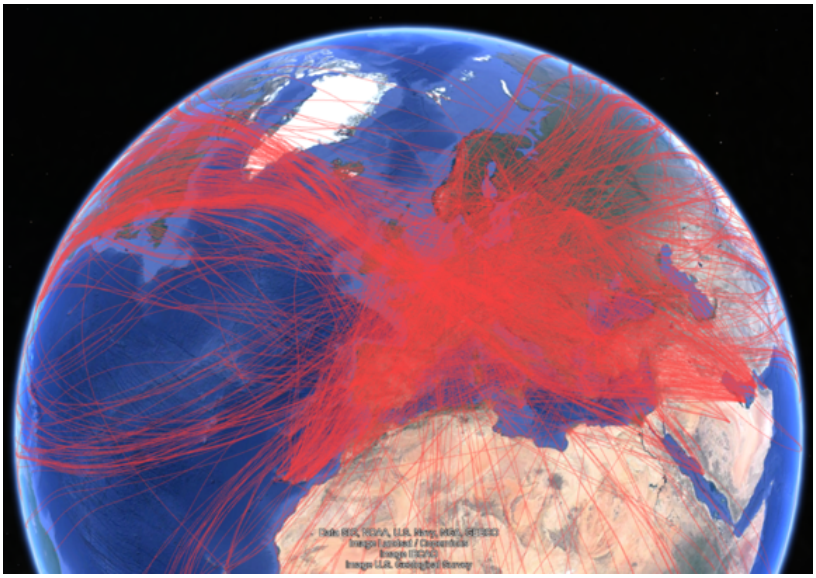


Figure 8 – Flights of the summer scenario day (June 16^{th}, 2018)

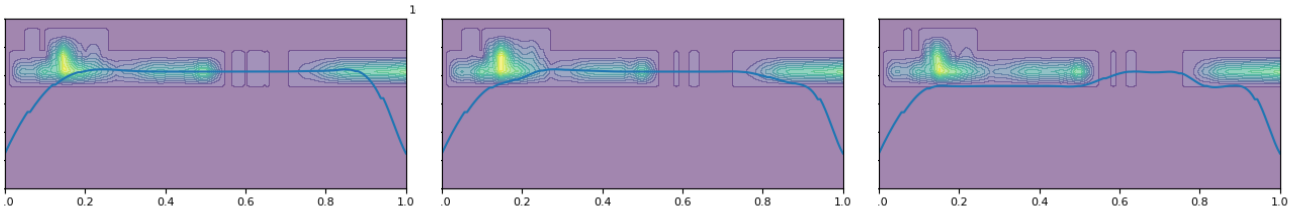
The days were chosen as they contain both climate sensitive regions, especially due to areas in which warming CiC form, and significant convective weather. Thus, they allow for checking if deconfliction will counteract the benefits of trajectory optimization. Although the aCCFs are partially used off-design, i.e. in regions they were not calibrated for, these scenario days help in understanding the interaction between trajectory optimization and subsequent deconfliction.

4. Results

4.1 Individual Trajectory Optimization

The individual trajectories were optimized to avoid convective cells while minimizing both DOC and climate impact. Although avoiding convective cells is imperative, the optimization allows for a trade-off between minimizing DOC and reducing climate impact.

As an example for the optimization of a single trajectory, Figure 9 shows three vertical profiles for flights from Barcelona (BCN) to Berlin (BER), flown by a Boeing 737-800. In Figure 9a, the trajectory is optimized with respect to DOC only. Here, the trajectory crosses areas in which warming CiC are forming. In Figure 9b, the optimization is mainly focused on minimizing DOC, while still reducing the overall non-CO_2 climate effect, implemented by using a numerically rather small weight for the climate impact, whereas in Figure 9c, the focus is shifted towards minimizing the climate effect.



(a) DOC-optimized

(b) Optimized considering non-CO_2 climate effect, but main focus on DOC.

(c) Stronger focus on climate impact

Figure 9 – Vertical profiles of flight trajectories from BCN to BER (B737-800)

In the case of DOC-optimization, the trajectory quickly reaches a height of approximately 10000 meters, which allows for both fast and fuel efficient flying. However, as areas in which warming CiC form are not considered in the optimization, large parts of the flights cross these areas. The result is shown in Table 1: While the fuel burn is low, the climate effect due to CiC, measured as F-ATR-50, is 885 pK.

Table 1 – Example for the interplay of climate optimization and fuel burn

Optimization Target	CiC Impact $[10^{-12}K]$	Fuel Burn [kg]	Flight Time [s]
DOC	885	4846	5961
mainly DOC	548	4906	5949
mainly climate	0.3	5172	5927

In the next case, the climate impact is considered in the optimization, but its weight in the multi-objective target function is low. However, as can be seen in Figure 9b, this suffices to move the trajectory to the border of the climate sensitive regions. The climate impact due to CiC is reduced from 810 pK to 548 pK, while the fuel burn is increased by 60 kg. A higher weighting of the climate impact in the objective function results in an additional downward shift of the trajectory, moving it further away from the climate sensitive regions. The climate impact due to CiC is almost eliminated, as it is reduced from 885 pK to 0.3 pK. However, the fuel burn is 5172 kg, an increase of 326 kg compared to the DOC-optimized case. Interestingly, the flight time is reduced by 34 seconds, as the maximum mach number allowed on this trajectory equates to a higher ground speed when the aircraft flies lower.

While the optimization of individual trajectories itself is an interesting and active field of research, we consider it in the perspective of an integrated scenario. Here, it means that flight times may be increased or decreased when the respective trajectories are optimized for their climate impact. Furthermore, clusters may emerge in which multiple flights are assigned to the same altitude, as this simultaneously minimizes costs and lies just below climate-sensitive regions. While optimal for each individual trajectory, this may be challenging when trying to assure that separation minima are not violated.

4.2 Deconfliction

Minimizing costs and reducing the climate impact of flights is important, but safety has the highest priority. While the individual trajectories are optimized such that each of them individually is safe, e.g. convective cells are avoided, there may be violations of separation minima between them. Thus, the individually optimized trajectories were checked for such conflicts. Table 2 shows the conflicts after the initial optimization step (O) for the scenario day 18th of June 2018.

Here, 962 conflicts occur. When the conflict resolution between the optimized trajectories is solved (optimized & resolved, OR), there are no more conflicts left, independent of the way of conflict resolution: Baseline (both time-based and lateral) or only time-based or lateral. After a second round of optimizations (ORO), new conflicts are created. However, the number of conflicts is lower than after

Table 2 – Comparison of deconflicting strategies in an iterative approach

Scenario	Optimization	Avg. Conflicts	Distance [NM]	Avg. Fuel Burn [kg]
Baseline	O	962	1491.1	15251
	OR	0	1491.1	15251
	ORO	211	1490.9	15250
	OROR	0	1490.9	15250
Time-Based Resolution	O	962	1491.2	15251
	OR	0	1491.2	15251
	ORO	220	1491.1	15251
	OROR	0	1491.1	15251
Lateral Resolution	O	962	1491.2	15251
	OR	0	1491.2	15251
	ORO	216	1491.1	15251
	OROR	0	1491.1	15251

the first iteration. In a second iteration (OROR), all these conflicts can be removed. Both the average distance over ground and the average fuel burn are hardly changed by this process, the average distance over ground differs by 0.01% between the approaches. Interestingly, the distance over ground is reduced by this process. This does not necessarily imply that the individually optimized trajectories were inefficient, as e.g. wind-optimized trajectories may be longer than the great circle between origin and destination. However, the fuel burn remains almost unchanged by this procedure.

4.3 Scenario Results

It is not surprising that the average fuel burn and, accordingly, CO_2 emissions of the optimized trajectories were changed only to a low extent, as the deconfliction procedure tries to resolve conflicts with small modifications of the trajectories.

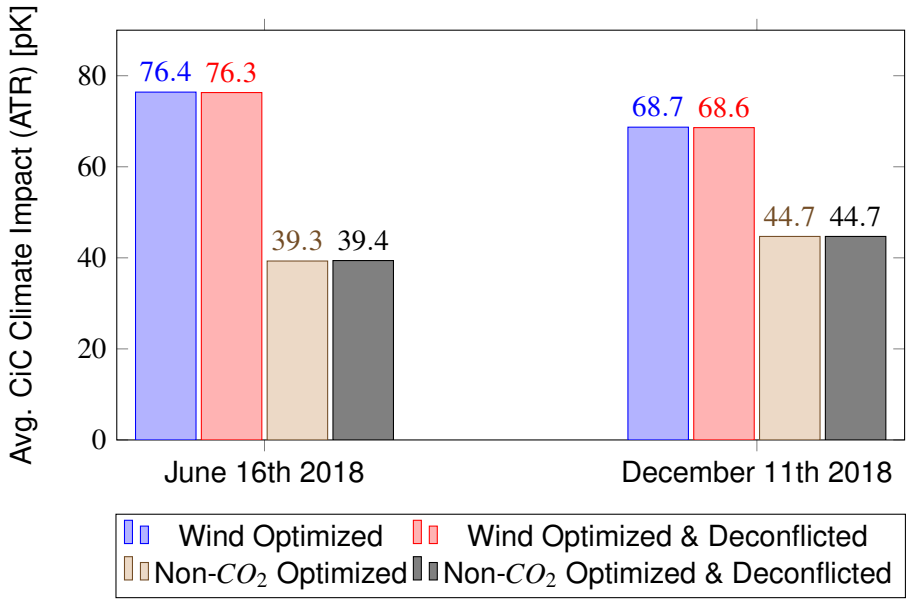


Figure 10 – Impact of Deconfliction on non-CO_2-effects of trajectories

Interestingly, this is also true for the non-CO_2-effects caused by CiC, as shown in Figure 10. For the scenario day June 16^{th}, 2018, the average climate impact of each trajectory caused by contrail-induced cirrus clouds is 76 pK, if these trajectories were only optimized for wind. This value does not change when conflicts are resolved. When non-CO_2-effects are also considered in the optimization,

the average climate due to CiC is reduced to 39.3 pK, which does not change after deconfliction. This result also holds for the winter scenario day: the average climate impact due to CiC is reduced from 68.7 pK to 44.7 pK, which remains stable after deconfliction. It is possible to run further iterations of optimizing the trajectories and deconflicting them, but as these results indicate one single "optimize first, deconflict later"-step is sufficient.

5. Conclusion

In a free-flight scenario, a sequential approach of optimizing trajectories and subsequently resolving conflicts was demonstrated to be feasible. As it was not clear to which extent the deconfliction process would degrade the efficiency gained by the trajectory optimization, whereas the optimiation would create new separation minima violations, this was designed as an iterative approach. However, it was shown that a single iteration is sufficient to minimize the climate impact, and resolve all conflicts. This was demonstrated with respect to the climate impact caused by contrail-induced cirrus clouds. However, another important factor in the non-CO_2-effects of aviation is the emission of NO_X, which can cause cooling effects by the reduction of methane in the atmosphere as well as warming effects by the increase in ozone. It is harder to optimize trajectories for reducing the NO_X-induced climate impact, as the gradients are not as step as it is the case for contrails-induced cirrus clouds, as shown in Figure 4b. This is an active area of research, and being investigated in the project "Flying ATM for Environment Impact" [1].

While this approach represents an initial step toward the operational use of climate-optimized trajectories, several challenges remain. Accurate forecasts of climate-sensitive regions are necessary to ensure that these areas are correctly predicted and that trajectory deviations effectively reduce the associated climate impact. Furthermore, fully implemented free-flight operations are not yet available at all times or across all airspaces. In current air transportation systems, aircraft are typically constrained to a fixed route network, which, while operationally advantageous, may limit the potential for mitigating non-CO_2 effects. This also accounts for vertical profiles, forcing aircraft to full flight-levels according to semicircular rules nowadays. Achieving practical implementation of climate-optimized trajectories therefore requires a holistic approach that considers not only trajectory optimization but also operational constraints, forecasting uncertainties, and conflict resolution. In this work, we follow a stepwise strategy, gradually increasing the realism of our modeling framework to bridge the gap between conceptual optimization and real-world applicability.

6. Contact Author Email Address

The contact author email address is Thorsten.Ehlers@dlr.de

7. Copyright Statement

The authors confirm that they, and/or their company or organization, hold copyright on all of the original material included in this paper. The authors also confirm that they have obtained permission, from the copyright holder of any third party material included in this paper, to publish it as part of their paper. The authors confirm that they give permission, or have obtained permission from the copyright holder of this paper, for the publication and distribution of this paper as part of the ICAS proceedings or as individual off-prints from the proceedings.

References

[1] Mendiguchía Meuser M, Lührs B, Linke F, Gollnick V, Matthes S, Dietmüller S, Baumann S, Soler M, Simorgh A, Yin F, and Castino F. Mitigation of aviation climate impact through robust climate optimized trajectories in intra-european airspace. In *Proc ICAS 2022*, 2022.

[2] Castino F, Yin F, Grewe V, Yamashita H, Matthes S, Dietmüller S, Baumann S, Soler M, Simorgh A, Mendiguchía Meuser M, Linke F, and Lührs B. Decision-making strategies implemented in solfinder 1.0 to identify eco-efficient aircraft trajectories. *Geoscientific Model Development*, 17(9):4031–4052, 2024.

[3] Mendiguchía Meuser M, Ehlers T, Lau A, Lührs B, Gruna R, and Kanitz R. pytom: A python-based multicriterial optimization framework for aircraft trajectories in large traffic scenarios. In *Proc 15th EASN International Conference*, 2025.

[1] https://www.f4eclim.eu/

[4] Alexander Kuenz. *High Performance Conflict Detection and Resolution for Multi-Dimensional Objects*. PhD Thesis, October 2015.

[5] Lee D S, Fahey D W, Skowron A, Allen M R, Burkhardt U, Chen Q, Doherty S J, Freeman S, Forster P M, Fuglestvedt J, Gettelman A, De León R R, Lim L L, Lund M T, Millar R J, Owen B, Penner J E, Pitari G, Prather M J, Sausen R, and Wilcox L J. The contribution of global aviation to anthropogenic climate forcing for 2000 to 2018. *Atmospheric Environment*, 244:117834, 2021.

[6] Yann Cohen, Didier Hauglustaine, Nicolas Bellouin, Marianne Tronstad Lund, Sigrun Matthes, Agnieszka Skowron, Robin Thor, Ulrich Bundke, Andreas Petzold, Susanne Rohs, Valérie Thouret, Andreas Zahn, and Helmut Ziereis. Evaluation of o3, h2o, co, and noy climatologies simulated by four global models in the upper troposphere-lower stratosphere with iagos measurements. *Atmospheric Chemistry and Physics (ACP)*, 25(11):5793–5836, 2025.

[7] Ziming Wang and Christiane Voigt. Tracing contrails within cirrus clouds and their climate effect. *Nature Communications*, 16(10702), November 2025.

[8] S. Matthes, K. Gierens, B. Beckmann, L. Bugliaro, S. Dietmüller, C. Frömming, M. Hanst, S. Hofer, J. Jene, S. Kirschler, C. G. Köhler, A. Lau, R. Leemüller, A. Liedtke, M. Mendiguchia Meuser, P. Peter, V. Santos Gabriel, I. Köhler, G. Saueressig, L. Schlemmer, J. Sperling, S. Schlobach, R. Schultz, K. von Sack, and N. Waltenberg. D-kult: data and tools for routine eco-efficient flight operations. *Journal of Environmentally Compatible Air Transport System Discussions*, 2026:1–40, 2026.

[9] F. Yin, V. Grewe, F. Castino, P. Rao, S. Matthes, K. Dahlmann, S. Dietmüller, C. Frömming, H. Yamashita, P. Peter, E. Klingaman, K. P. Shine, B. Lührs, and F. Linke. Predicting the climate impact of aviation for en-route emissions: the algorithmic climate change function submodel accf 1.0 of emac 2.53. *Geoscientific Model Development*, 16(11):3313–3334, 2023.

[10] Dietmüller S, Matthes S, Dahlmann K, Yamashita H, Simorgh A, Soler M, Linke F, Lührs B, Mendiguchía Meuser M, Weder C M, Grewe V, Yin F, and Castino F. A python library for computing individual and merged non-co2 algorithmic climate change functions: Climaccf v1.0. *Geoscientific Model Development*, 16(16):4405–4425, 2023.

[11] Matthes S, Dietmüller S, Dahlmann K, Frömming C, Peter P, Yamashita H, Grewe V, Yin F, and Castino F. Updated algorithmic climate change functions (accf) v1.0a. *Geoscientific Model Development Discussions*, pages 1–28, 2023.

[12] Niklaß M, Lührs B, Grewe V, Dahlmann K, Luchkova T, Linke F, and Gollnick V. Potential to reduce the climate impact of aviation by climate restricted airspaces. *Transport Policy*, 83:102–110, 2019.

[13] Lau A, Ehlers T, Derra M, and Lührs B. Considerations for multi-criteria route design on different atmospheric scales. In *Proc ICAS 2022*, 2022.

[14] Hersbach H, Bell B, Berrisford P, Hirahara S, Horányi A, Muñoz-Sabater J, Nicolas J, Peubey C, Radu R, and Schepers D. The era5 global reanalysis. *Quarterly Journal of the Royal Meteorological Society*, 146(730):1999–2049, 2020.

[15] Zinner T, Mannstein H, and Tafferner A. Cb-tram: Tracking and monitoring severe convection from onset to mature phase. *Meteorology and Atmospheric Physics*, 101(3):191–210, 2008.

[16] Tansel Uras and Sven Koenig. An empirical comparison of any-angle path-planning algorithms. *Proceedings of the International Symposium on Combinatorial Search*, 6(1):206–210, Sep. 2021.

[17] Kenny Daniel, Alex Nash, Sven Koenig, and Ariel Felner. Theta*: any-angle path planning on grids. *J. Artif. Int. Res.*, 39(1):533–579, September 2010.

[18] Nuic A, Poles D, and Mouillet V. Bada: An advanced aircraft performance model for present and future atm systems. *International Journal of Adaptive Control and Signal Processing*, 24(10):850–866, 2010.

[19] Falck R, Gray J S, Ponnapalli K, and Wright T. dymos: A python package for optimal control of multidisciplinary systems. *Journal of Open Source Software*, 6(59):2809, 2021.

[20] Kuenz A. Free vertical planning in a tbo environment. In *44th IEEE/AIAA Digital Avionics Systems Conference (DASC 2025)*, 2025.

[21] Kuenz A, Lau A, Ehlers T, and Sanaei R. Weather-optimized individual routes in a global scenario. In *Proc IEEE/AIAA 42nd Digital Avionics Systems Conference*, pages 1–8, 2023.